Silicon Nanomembranes for Rapid Liquid Biopsies From Whole Blood and Urine

Thesis Proposal

Kilean Lucas

Advisors

Prof. James McGrath

Prof. Richard Waugh

Committee

Prof. Ed Brown

Prof. Stephen Dewhurst

Prof. Benjamin Miller

Exam Chair

Prof. Lisa DeLouise

December 20, 2017

TABLE OF CONTENTS

SPECIFIC AIMS

Americans have a 33% chance of developing cancer and a 20% chance of dying from cancer [1]. Late stage cancers are genetically diverse tumors that are resistant to any particular treatment [2, 3]. The diagnosis of cancer in its earliest stages would result in annual U.S. health care savings over $300B [3]. Because early cancers are often asymptomatic, they are difficult to diagnose. The ideal early detection assay should be non-invasive, sensitive, and affordable enough to be used in routine care. This is the goal of the 'liquid biopsy' – a still theoretical diagnostic assay, which uses a small volume of body fluid to identify cancers at their earliest stages. The discovery that exosomes, 30-150 nm diameter lipid vesicles that are secreted by most cells and accumulate in body fluids, carry molecular markers of cancer and other diseases [4-6] has made them a promising target for liquid biopsies [7]. Exosomes bearing disease-related markers are rare however (< 1% of the total) [8, 9], and thus techniques that isolate exosomes with high yield and purity are necessary for liquid biopsies. The most common purification methods [7, 10, 11] require large volumes (50 – 300 mL) of fluid and multiple, labor-intensive steps such as ultracentrifugation and size-exclusion chromatography. More convenient techniques such as PEG co-precipitation and spin-column filtration co-purify exosomes with protein contaminants [12], which limits the ability to use exosomal protein as a biomarker. In this thesis, I propose to develop tangential flow microfluidic devices featuring ultrathin silicon membranes (nanomembranes) for the rapid isolation of exosomes from raw biofluids and the *in situ* identification of cancer biomarkers.

Aim 1: Develop dynamic and static analytical models that are predictive of exosome capture to optimize flow conditions. This Aim will combine computational modeling and model experiments to identify optimum conditions for exosome capture by nanomembranes in microfluidic devices. In the dynamic model, COMSOL Multiphysics will predict fluid streamlines for a range for tangential flow rates, transmembrane flow rates, and channel heights, which we will then superimpose on Brownian motion simulations of exosome diffusion. Capture will be assumed to occur when the combination of Brownian and convective motion brings exosomes to within an exosome diameter of the membrane provided that the criteria for stable capture determined by the statics mode is met. These simulations will predict the fraction of exosomes captured in one pass through the device assuming a source concentration of ~10^9 per mL. We will test these predictions with experiments employing gold nanoparticles as exosome surrogates and revise modeling and experiments until a predictive model is identified. *The goal is to identify conditions for the capture of > 7.5 x 10^8 nanoparticles from a starting volume of 1 mL with ~10^9 total nanoparticles (> 75% capture).*

Aim 2: Develop a tangential flow microfluidic filtration system for isolating components of blood and urine. Here we will apply the optimized flow conditions of Aim 1 to maximize the capture of exosomes from undiluted blood and urine. Whole blood will first be fractionated using a combination of microporous and nanoporous silicon nanomembranes to generate plasma. Starting exosome concentrations will be calculated from optical particle counts (nanoparticle tracking analysis or NTA) in the purified samples. Capture efficiency will be determined by counting exosomes *in situ* (by electron microscopy) and by eluting exosomes from membranes with a backwash and counting them in the collected volume (by NTA). *Success will be the demonstration of a capture efficiency > 75% of the total exosomes from both biofluid samples.*

Aim 3: Demonstrate the ability to identify cancer-derived exosomes from non-cancer exosomes *in situ* on a silicon nanomembrane. Here we will use nanomembrane microdevices to identify tumor-derived exosomes *in situ*. We will purify exosomes from tumorigenic and non-tumorigenic urinary cell lines and mix them at ratios of 1:100; 1:1,000; 1:10,000; to 1:10^6 to a final concentration of 10^9 /mL. Nanomembrane chips will be extracted from devices and exosomes will be labeled for the bladder cancer (BC) biomarker MUC2 and scanned by optical microscopy (fluorophore-tagged antibodies) and electron microscopy (gold-tagged antibodies). *Success will be identification of samples containing MUC2 positive exosomes diluted in a population of MUC2 negative exosomes (1:1000 ratio or better).*

SIGNIFICANCE

Exosomes are 50 – 150 nm extracellular vesicles secreted by most cells. While they have a physiological role as carriers of molecular information between cells [13, 14], they are also prime targets for early cancer diagnostics because: 1) they carry molecular markers of their cell-of-origin including tumors [4-6], and 2) they are found in abundance ~10^9 /mL in most body fluids [15] (e.g. urine, blood, CSF). Because early cancers are often asymptomatic, detection assays should be non-invasive, sensitive, and affordable enough to be part of a blood panel or urinalysis done in regular check-ups. With this goal in mind, this proposal will focus on the isolation of exosomes from blood and urine.

Blood has been used as a source of diagnostic information for centuries [16]. As blood interacts with all tissues in the body, it samples and accumulates particles and exosomes from a wide variety of cells. Circulating exosomes containing tumor-derived microRNA isolated from human serum have been used with 72% specificity to identify patients with lung adenocarcinoma vs. healthy patients [17]. Moon, et al. have shown that the plasma-derived exosomes of patients with breast cancer express the developmental endothelial locus-1 protein (Del-1), which was not found on the exosomes of healthy patients, facilitating the early diagnosis of breast cancer [18]. Ovarian cancer microRNAs have been identified in exosomes from patient plasma samples with 70-90% correlation with cell-derived microRNAs [19].

In contrast to the diverse collection of exosomes found in blood, biomarkers on urinary exosomes are primarily sought for their potential to diagnose bladder cancer (BC). Bladder cancer is the 5th most common malignant cancer [1] and the most expensive to treat because of its high rate of recurrence requires regular invasive surveillance over the lifetime of a patient [20]. Chen et al. first identified 22 discrete proteins in the urinary exosomes of bladder cancer (BC) patients not found in healthy volunteers and several markers distinguishing low grade bladder cancer (LBGC) from high grade bladder cancer (HGBC) [21]. Beckham et al. discovered that EDIL-3 is enriched in urinary exosomes from patients with HGBC [22]. Armstrong et al. [23], analyzed miRNA from patient-matched tumor tissue and urinary exosomes to discover that a significant overlap in miRNA profiles.

The “gold standard” method for isolating exosomes from biofluids is ultracentrifugation, which requires large volumes of biofluid (> 25 ml), long processing times, expensive instrumentation and trained technicians. Gel precipitation, size exclusion chromatography, and affinity capture kits have been developed that remove the need for ultracentrifugation and allow exosome isolation in a benchtop centrifuge [24-27], but these methods suffer from low yield and contamination with co-precipitated proteins [24, 26, 28]. The high protein contamination from these methods prevents the use of exosomal proteins as biomarkers in addition to RNA. Microfluidic techniques exist for capturing exosomes, often employing size or affinity to separate exosomes, but these techniques are complex [29], have poor yields (2%, [30]), and require pre-processing of the sample to remove cellular components [19, 29, 31]. With tumor-derived exosomes constituting < 1% of the total exosome population [8, 9], the yield of exosomes that results from current microfluidic methods will make it difficult to detect scarce biomarkers. For a liquid biopsy to be widely adopted, it should be simple and quick to use, capture the majority of exosomes from a small sample of biofluid in a manner that enables the identification of both protein and RNA-based biomarkers on a subpopulation of the total exosome population.

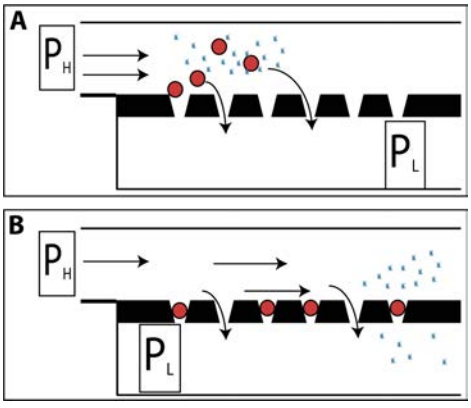

Figure 1: A) Capture of exosomes from an undiluted biofluid in the pores of a nanomembrane is governed by the transmembrane pressure. B) Captured exosomes can be “washed” of protein to purify them.

We have discovered that silicon nanomembranes - an ultrathin nanoporous platform developed and refined in Rochester over the last decade - capture exosomes in

individual pores when raw biofluid is passed tangentially over the membranes. This simple exosome capture is enabled by the high permeability nanomembrane and the fact that nanomembrane pores have the same dimensions as exosomes. Tangential flow allows clearance of cell debris and protein contaminants while providing transmembrane pressure to enable capture (**Figure 1**). Once this technique has been refined, it will open the door to easy to use and rapid assays for diagnosing cancer at early stages. Our contribution will bridge the gap between semi-automated microfluidic platforms with complex designs (e.g. nanoscale lateral displacement arrays [32]) and relatively simple but labor intensive approaches (e.g. ultracentrifugation) for the capture of exosomes from biofluids.

INNOVATION

A key innovation of this proposal lies in our use of ultrathin silicon nanomembranes as the basis for exosome isolation from complex fluids. One unique property of silicon nanomembranes is the ability to tune pore diameters to provide size cutoffs that match the size of the exosomes. This enables us to capture exosomes in high densities within the pores, rather than on top of the pores or in the filtrate (**Figure 2A**). In-pore capture facilitates a platform for exosome-by-exosome analysis of the sample with high resolution imaging techniques (e.g. electron microscopy or super resolution optical microscopy). This may be advantageous for early detection, where tumor derived exosomes may be in concentrations that are too low for Western blot (~1 μg of exosomal protein is considered the minimum detectable limit for positive identification [33]) or dot blot (~ 5 ng of CD63 [34]) detection.

In-pore capture of exosomes coupled with tangential flow minimizes protein contamination. This is particularly important for purification from human plasma, which is rich with protein (> 60 mg/mL [35]). In normal flow, plasma quickly fouls membranes in the form of a thick cake layer that dwarfs the membrane (**Figure 2B**). However, by flowing the sample tangential to the surface of the membrane, we can capture exosomes from undiluted human plasma with minimal protein contamination (**Figure 2A**). The shear induced by the tangential flow will reduce levels of circulating protein on the membrane surface, but exosomes will remain on the membrane due to a combination of the transmembrane pressure and the in-pore capture process.

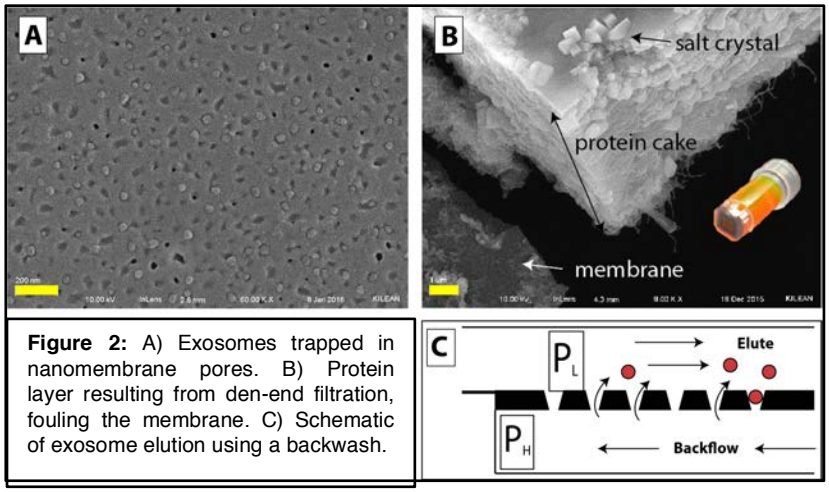

Figure 2: A) Exosomes trapped in nanomembrane pores. B) Protein layer resulting from den-end filtration, fouling the membrane. C) Schematic of exosome elution using a backwash.

Because exosomes captured on nanomembranes are spatially separated at high densities (~100 nm apart), in situ identification of biomarkers on individual exosomes should be possible with appropriate detection tools. Moreover, with low protein contamination in tangential flow, robust cancer diagnostics may be achieved through the simultaneous identification of surface protein and microRNA (miRNA) biomarkers. In addition to in situ identification of biomarkers, it should be possible to lyse exosomes on the membrane and capture the lysate, or elute exosomes via a simple backwash (**Figure 2C**). This last approach would enable the traditional molecular analysis of exosomes via PCR and Western blotting, but with far less contaminating protein. Thus nanomembranes provide a range of new opportunities for the capture, purification of exosomes from undiluted biofluids and the detection of associated biomarkers.

APPROACH

The goal of this project is to develop a platform to capture and detect cancer-derived exosomes from small volumes of whole blood and urine. Our guiding hypothesis is that tangential flow microfluidics combined with the unique properties of ultrathin silicon nanomembranes will allow for the capture of exosomes with high yield and purity. We additionally hypothesize that the unique ability of

nanomembranes to capture and isolate exosomes at high density will allow for on-chip exosome-by-exosome analysis to identify tumor-derived exosomes in a background of 'normal exosomes'. We will test these hypotheses in three aims that begin with simple model systems (**Aim 1**), then move to more challenging biofluids (**Aim 2**), before finally testing with cancer-related samples (**Aim 3**).

Aim 1: Develop dynamic and static analytical models that are predictive of exosome capture to optimize flow conditions.

Rationale: The phenomena of exosome capture in our microdevices should be predictable from a knowledge of flow fields, channel geometries, membrane parameters (permeability, pore sizes), and exosome properties (size, concentration, diffusion coefficient). Thus we will develop predictive analytical and computational fluid dynamics (CFD) models of exosome capture assuming exosomes are rigid spherical particles. A static model will be developed to identify conditions that give stable particle/pore association (**Figure 3A**). A dynamic model (**Figure 3B**) will be developed to predict capture efficiencies and optimize flow conditions to achieve > 75% capture in a single pass over the membrane. The models will be tested using gold nanoparticles as surrogates for exosomes. The density of gold makes assessment of capture by electron microscopy very easy.

Static Model of Exosome Capture on Pores:

A static force balance governs particle retention on a pore. This balance determines whether the particle will be retained under flow or if it will be dislodged from the pore and swept downstream. Mechanical balance will occur if the downstream drag force – modeled as a modified version of Stokes' drag for a sphere near a wall [36] – is greater than the transmembrane force that pulls the particle down onto/into the pore (**Figure 3A**). The drag force is determined by the particle size and downstream velocity (calculated from the volumetric flow rate and the channel dimensions). The transmembrane pressure is determined by the flow rates above and below the membrane and the resistances of membrane and flow channels. Relating these effects as in **Figure 3A**, I have developed a preliminary static balance for particle capture that predicts the key relationship is:

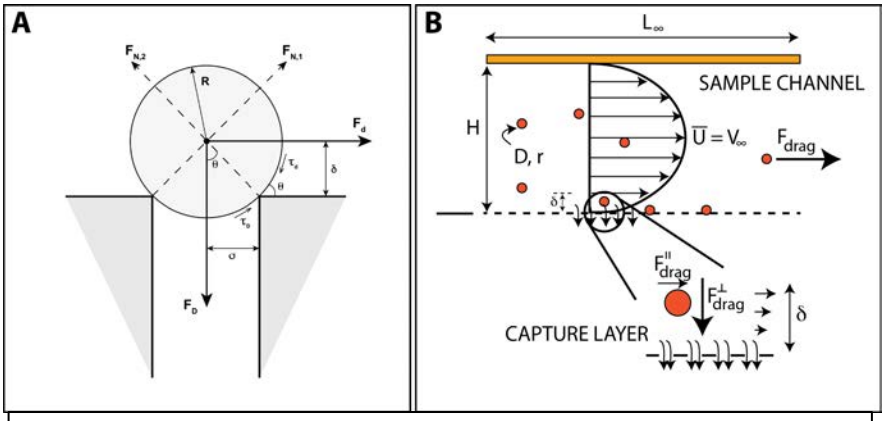

Figure 3: Mathematical model of a particle being captured by a pore. A) Static model of particle retention on the pore for determining the transmembrane pressure required to retain the particle. The downstream drag force (F_d) must be exactly balanced by the transmembrane force (F_D) in order for the particle to remain on the pore rather than being swept downstream. B) Dynamic model of particle motion towards the membrane under tangential flow. The particles must diffuse into a "capture layer" in which they will interact with the membrane and be captured.

$$\Delta P = \frac{F_D \cdot \frac{\delta - R\cos\theta}{\sigma - R\ \sin\theta}}{A_p} - \frac{m \cdot g}{A_p} \quad (1)$$

where A_p is the pore cross-sectional area and F_D is the modified Stokes' drag. The angle θ is given as:

$$\theta = \tan^{-1}\frac{\sigma}{R - \sigma} \quad (2)$$

which accounts for the separation distance between the center of the particle and the surface of the membrane. The stability of gold nanoparticles under these conditions will be verified using the final device design determined from the dynamic model.

Dynamic Model of Exosome Capture: The dynamic model of exosome capture will determine exosome trajectories in our microdevice by accounting for fluid convection and exosome diffusion. The model presumes that for particles to be captured, they must diffuse into a layer near the membrane that we define as a "capture layer" (**Figure 3B**). Particles in this capture layer can then be expected to experience forces that result in their capture on/in pores, provided that the conditions for stable particle retention from the static model are satisfied. By adjusting the flow rates in the top and the bottom channels (**Figure 4**), we can adjust the thickness of the capture layer as well as the pressure drop across the membrane. Using COMSOL Multiphysics, I have developed a computational model predicting streamlines and pressure drops across the membrane (**Figure 5A**)

Transmembrane Flow (μL/min) \ Sample Flow Rate (μL/min)	0.1	0.5	1	5	10	50	100
0	✔	✔	✔	✔	✔	✔	✔
0.5	✖	✖	✔	✔	✔	✔	✔
2	✖	✖	✖	✔	✔	✔	✔
10	✖	✖	✖	✖	✖	✔	✔

Figure 4: Proposed sample flow rates and transmembrane flow rates for gold nanoparticle capture trials. The transmembrane flow will be either passive (0 μL/min) or active (> 0 μL/min).

To understand particle motion in the fluid, we make the assumption that in the absence of diffusion, particles are small enough to follow the streamline they are on (**Figure 5B**). This allows us to avoid the drag calculation that would be needed to determine the trajectory of a particle that spans multiple streamlines. For very small particles far from the membrane, this assumption is valid, but may begin to lose its validity as the particles approach the membrane and span the capture layer, requiring further refinement of the dynamic model. Streamlines will be extracted from CFD simulations of flow and will be used as the basis for a MATLAB particle-tracking algorithm. Exosome trajectories will be determined by 'releasing' particles on the upstream part of the membrane at random heights above the membrane and adding a diffusive 'jump' to the convective displacement calculated for a small time interval. This will cause the particles to assume a trajectory that appears as a random walk that is biased by the streamline. The diffusive step in the two coordinate dimensions (x, y) is given by randomly sampling the normal probability distribution, given by:

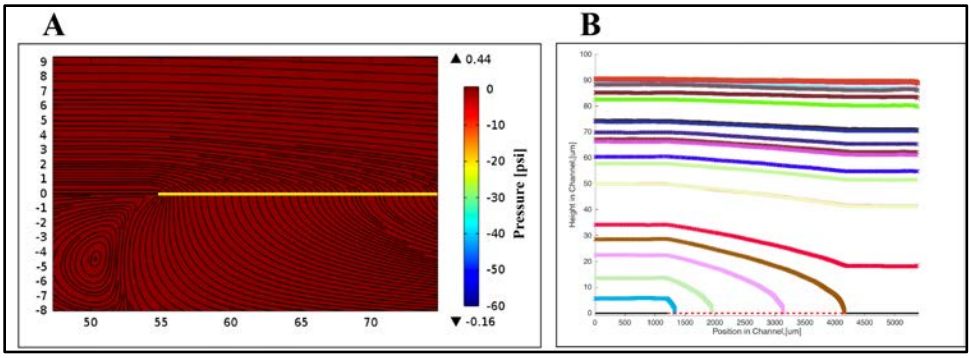

Figure 5: A) COMSOL Multiphysics model of transmembrane flow through a nanoporous silicon nitride membrane. The membrane is represented by the yellow line. There is no measureable pressure drop across the nanomembrane, indicating that conditions are appropriate to minimize shear. B) MATLAB particle tracking algorithm showing the tracks of twenty 50 nm particles in the system. With a flow rate of 10 μL/min on the top channel and an ultrafiltration rate of 2 μL/min, particles with the first ~30% of the membrane will be captured.

$$P(\Delta x, \Delta y) = \frac{1}{(4D\Delta t)^{1/2}} e^{\frac{-\langle \square^2 \rangle}{4D\Delta t}} \quad (3)$$

where $\langle x^2 \rangle$ is the mean squared displacement of the particle. The particle diffusivity, D, is given by the Stokes-Einstein equation for the motion of a particle:

$$D = \frac{k_B T}{6\pi \cdot \mu \cdot r} \quad (4)$$

where k_B is the Boltzmann constant, μ is the fluid viscosity and r is the particle radius. Because the streamline data is extracted from a CFD simulation, the velocity data is generated for each individual node. However, the diffusion calculation may position the particle where there is no velocity data, so the particle-tracking algorithm will adjust for this and position the particle at the nearest node. Mesh size will therefore be important in determining the coarseness of this adjustment. The time step is derived from the velocity of the fluid and is given as:

$$\Delta t = \frac{r}{V} \quad (5)$$

where V is the fluid velocity.

Simulations will be run over a range of: 1) flow rates in both top and bottom channels (0.1-100 µL/min top, 0-10 µL/min bottom), 2) channel dimensions (50-300 µm), 3) and exosome sizes (50-150 nm). The conditions span a range of Peclet numbers, *Pe*, from 10^{-2} to 10^{2} , where *Pe* is the ratio of residence time of particles above the membrane to diffusion time across the channel. While in principle smaller *Pe* numbers should give a greater chance of membrane encounter, they may also prescribe impractically long transit times. Thus the optimum flow conditions are not obvious without simulation.

Conditions associated with >75% pore occupancy during a single pass will be identified. This corresponds to 75% of 3 x 10^8 pores for one 2 mm x 0.7 mm membrane (a standard format) or 75% of 10^9 pores for three 3 mm x 0.7 mm membranes (a newer format). Importantly, the pressures and mean velocity of each simulation can be determined and compared to Equation 1, building a connection between the statics and dynamics models and providing design principles for our device.

Experimental Validation of the Models: Capture efficiencies for gold nanoparticles tuned to the average nanoporous nitride (NPN) pore size will be experimentally determined for each of the flow rates shown in Figure 4. The gold nanoparticles will be used at a concentration of 10^9 nanoparticles/mL which is the concentration of exosomes found in circulating blood [15]) and capture will be performed on a membrane chip with three 3 mm x 0.7 mm windows containing ~ 10^9 total pores total. The number of particles captured will be determined through scanning electron microscope (SEM) analysis of the membrane surface as well as through nanoparticle tracking analysis (NTA, NanoSight NS300) of the non-captured (top channel, post filtration) fraction. Preliminary experiments with 10^9/mL 60 nm gold nanoparticles in NanoPure water have only achieved 10% capture efficiency (**Figure 6A**). While this is significantly lower than our goal, we note that there has been no attempt at optimization yet.

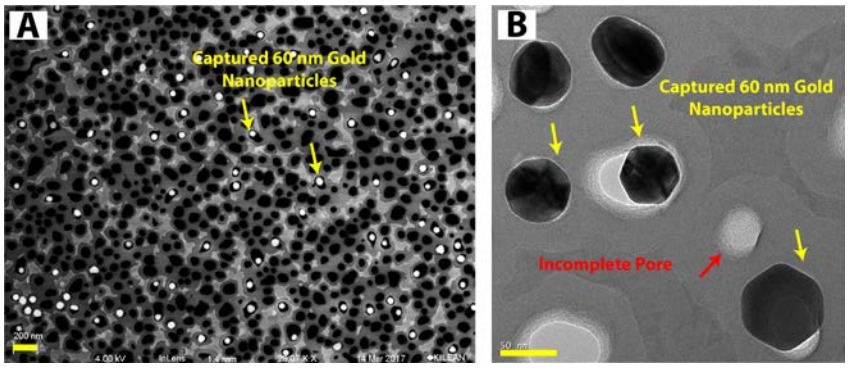

Figure 6: A) Gold nanoparticles (60 nm) captured on a silicon nanomembrane in tangential flow. The pore occupancy (capture efficiency) is approx. 10%. B) TEM of silicon nanomembrane with captured gold nanoparticles, the red arrows indicate occluded pores, which limit capture. Some membranes have a higher frequency of occluded pores, leading to membrane variability. Scale in A and B = 200 nm and 50 nm respectively.

Addition of Protein: To more accurately model capturing exosomes from human plasma and urine bovine serum albumin (BSA) will be added to the sample in increasing concentrations to simulate blood albumin (60 mg/mL [35]) and urine protein (2 mg/mL

[37]) levels. This is an important experiment as the protein may interfere with the capture of particles and affect our operating conditions for 75% capture.

Metrics for Success: This Aim will be successful if we: 1) develop a static model for the capture of particles that is predictive of stable capture in our experiments and 2) develop a dynamic model that successfully predicts capture of > 75% nanoparticles from a 1 mL solution with a starting concentration of 10^9 particles/mL.

Challenges and Alternative Strategies: There are a number of factors that cause discrepancies between our models and experiments. First, NPN membranes have a distribution of pore sizes, tapered pores, and some incompletely etched pores that are not available for capture (**Figure 6B**). A more accurate representation of pore distribution and geometry may be warranted to resolve discrepancies between model and experiments.

The addition of protein is likely to cause membrane fouling in at least parts of the flow regime associated with high rates of capture. For example if flow were strictly normal to the membrane, 100% of particles would be captured, but the protein would produce a thick cake layer (**Figure 2B**). Thus while we expect these model studies to provide guidelines, we fully expect the compromise between capture rate and purity will need to be optimized with real biofluids (**Aim 2**).

Exosomes are a polydisperse population and so representing them by a single, monodisperse nanoparticle system may prove insufficient when we move to real systems below. If needed we can revisit these models with a more accurate distribution of exosomes obtained from NTA measurements and revisit experiments with a custom mixture of gold nanoparticle sizes that model real exosome distributions.

Using the velocity to control capture for a system where the height of top channel is very small, may prescribe very high pressures. This could have two detrimental results: 1) the transmembrane pressure may be large enough that the membrane fails or the device leaks or 2) the pressures may cause damage to exosomes.

The model is based on a rigid sphere assumption that does not capture the deformability of biological membranes, and this deformability may determine particle positions and stability in a pore. Additionally, the tapered pore shape of NPN membranes may need to be investigated as this may provide additional stability if particles are lodged deep in a pore.

Aim 2: Develop a tangential flow microfluidic filtration system for isolating components of blood and urine.

Rationale: With the identification of conditions that give > 75% particle capture in **Aim 1**, we will now apply those conditions to real biofluid samples. Whole blood and urine are the optimal choices for a biofluid as they: 1) are obtained through minimally invasive procedures as part of routine medical care and 2) contain exosomes with promising cancer biomarkers. The two fluids are also on opposite ends of the complexity spectrum for biofluids with urine being mostly cell free and low in protein content (< 2 mg/mL [37]), while blood is rich in both cells and protein. Filtering blood to create plasma without activating or lysing cells will be one of the challenges of the blood sample. Capturing exosomes at high efficiency while minimizing protein fouling or contamination will be another challenge with blood. If these challenges prove too difficult to meet, we should still expect success with far simpler, but still clinically relevant, urine samples.

Aim 2a: Capture 75% of exosomes in 1 ml of undiluted blood plasma using nanoporous silicon nitride nanomembranes in a tangential flow microfluidic device.

Plan: Using flow conditions identified by the model systems of Aim 1, we will operate our tangential flow microfluidic device to capture exosomes from whole blood plasma (**Figure 7a**). To test capture efficiency, we will first use exosomes that have been purified by the traditional ultracentrifugation method [31]. We will characterize these exosomes using Western blot for common exosome markers

(e.g. Tsg101, Alix, CD63) as well as nanoparticle tracking analysis (NTA, NanoSight NS300) to determine identity and concentration. We will then capture the exosomes from 1 mL of sample on the membrane using the flow conditions determined in **Aim 1** and characterize the capture efficiency using SEM. Additional characterization will be done by washing with 1x Hank's Balanced Salt Solution (HBSS), followed by backwash (**Figure 2C**) of the collected samples and analysis with NTA.

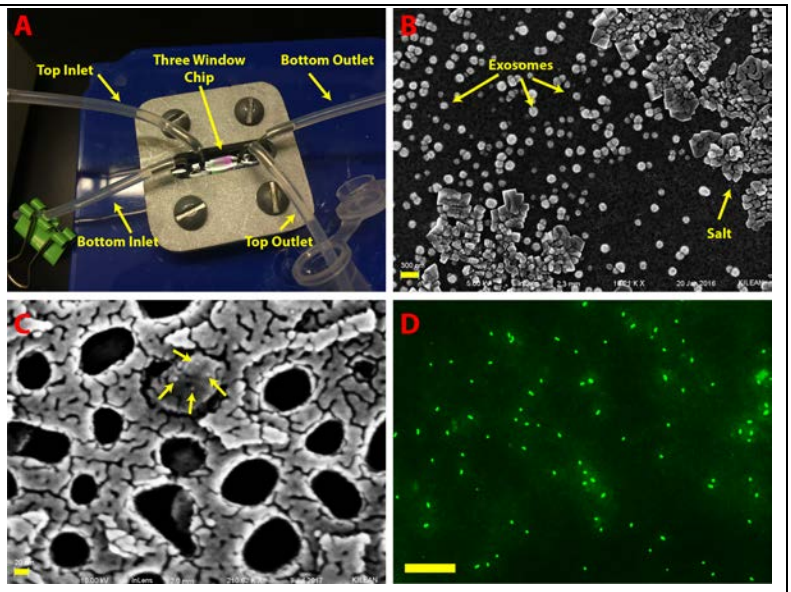

Figure 7: A) Tangential flow microfluidic device for exosome separation. The bottom outlet is blocked to generate a pressure drop across the membrane. B) Exosomes and salt from undiluted whole blood on a silicon nanomembrane. Scale = 300 nm. C) CD63 immunogold (10 nm) labeled exosome captured in the pores of the nanomembrane. Scale = 20 nm. D) Purified exosomes captured on the membrane labeled with SYTO RNAselect dye. Scale = 1 µm.

After using purified exosomes to confirm the capture process, we will then use 1 mL of whole, undiluted human plasma (Equitech-Bio, Kerrville, TX) to increase the sample complexity. The sample will be used in the device the same way as the purified samples and will be further characterized for protein contamination using x-ray photoelectron spectroscopy (XPS). We have developed a novel technique to characterize the thickness of protein layers on our nanomembrane surface [38] and we will apply this technique to quantifying the level of protein contamination *in situ*. It has been shown that ultracentrifugation of human plasma yields an 'impure' exosome population (< 10^{10} exosomes/µg protein) [12] and we can compare our method of isolation to the conventional methods with the expectation that we will exceed this standard. Exosomes captured from plasma will be characterized using the same techniques as for purified exosomes (see previous paragraph), with the addition of using a RNA selective dye (SYTO RNAselect, Thermo Fisher Scientific) to confirm the identity of the exosomes *in situ* using fluorescence microscopy (**Figure 7D**).

Metrics for Success: This Aim will be validated by: 1) capturing > 75% (of an expected concentration of 10^9 exosomes/mL) of the exosome population from whole plasma and 2) achieving a purity > 10^{10} exosomes/µg protein for exosomes captured on nanomembranes.

Progress: Initial experiments performed using undiluted human plasma obtained (Equitech-Bio) have established that we can successfully capture exosome-sized particles on nanomembranes (**Figure 7B**). Furthermore, using immunogold identification *in situ* we have shown that these particles are positive for CD63, a common exosome marker (**Figure 7C**). Capture from the purchased plasma sample has been replicated with varying degrees of success, thus motivating the need to refine the flow conditions and maximize efficiency. Work with samples of concentrated purified exosomes (~ 10^{10} /mL) has shown that we can obtain capture density exceeding the pore density of the membrane (**not shown**).

Preliminary protein contamination studies have been carried out where we compare the purity of exosomes isolated in normal flow (in a standard centrifuge filtration setup) with those isolated from whole plasma in tangential flow and by ultracentrifugation and deposited on our membranes (**Figure 8**). In order to compare data between samples in the XPS, we have to analyze the carbon to silicon (C:Si) peak ratio as the counts per sample vary quite significantly.

Conclusions: Exosome capture in tangential flow has been successfully demonstrated, though not optimized. Additionally, it has been shown that exosomes have been isolated by tangential flow on

silicon nanomembranes have a lower protein content than exosomes that have been isolated using ultracentrifugation.

Remaining Work: The work that remains in this Aim is to develop a more repeatable method of isolation that demonstrates consistent capture efficiency > 75% from whole plasma as well as to further investigate protein contamination using biological replicates (n = 3). Furthermore, we need to characterize fluorescent labeling of exosomes for *in situ* characterization and visualization of capture while the experiment is running, so that we avoid potential drying artifact from the preparation for SEM.

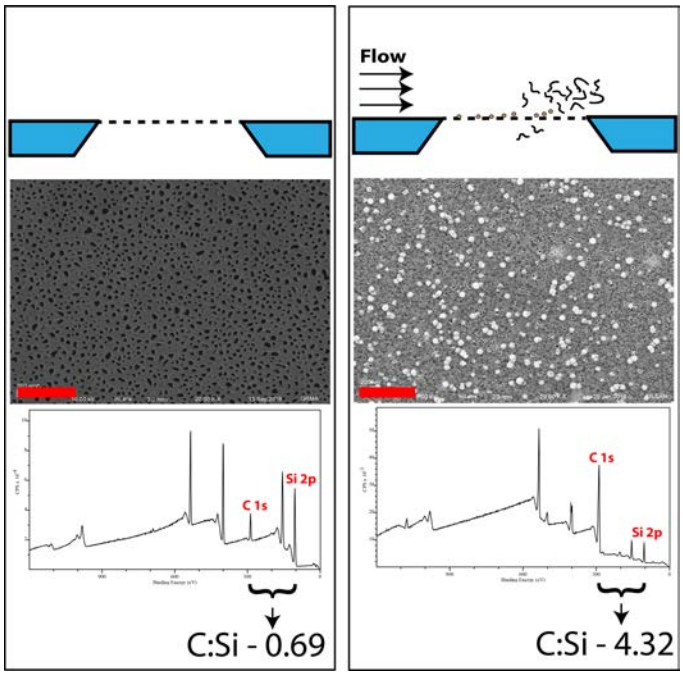

Figure 8: XPS analysis of protein contamination. Comparison of a clean membrane and a membrane used to filter undiluted plasma in tangential flow with visible exosomes. The C:Si ratio indicates the thickness of a contamination layer or exosome layer on the membrane. The C:Si ratio is also visible as a peak ratio in the XPS spectra. Scale bars = 1 µm.

Aim 2b: Develop a tangential flow device that removes the cellular component of whole blood to produce plasma

Plan: With the ultimate goal of producing a system capable of extracting exosomes from whole blood, we must also develop a device that produces plasma by removing all cellular components. This device could operate 'upstream' of the exosome extraction device of **Aim 2a**.

Using microporous membranes, we will separate white blood cells (WBCs) from whole blood and then red blood cells (RBCs) and platelets to produce plasma. We will explore the flow conditions of **Aim 1** (**Figure 4**) to optimize the removal of 99% of the cellular material from a small volume (~ 200 µL) of whole blood. To accomplish this, we will use microporous 'slit' membranes that have pores (slits) 2 µm in width (50 µm in length) to separate the WBC population followed by an additional microporous slit membranes with 0.4 µm pores to remove the RBC and platelet populations. Slit membranes have the selectivity of circular pores, but higher throughput [39].

Whole blood samples will be obtained by venipuncture from consenting donors and collected in a tube treated with sodium citrate. The blood sample will be loaded into a vertical reservoir (**Figure 9a**), which will account for cell settling and the flow conditions deemed appropriate for capture in **Aim 1** will be applied. To characterize the separation efficiency, we will use SEM as well as perform a hemocytometer analysis of both the filtrate and retentate fractions with platelets being identified by anti-CD41 targeted staining. To positively identify white blood cells in the hemocytometer, we will stain with the Hoechst DNA dye. Stressed RBCs will be identified by visual inspection of retained and filtered RBCs for signs of echinocytosis. The integrity of RBCs will be confirmed by measuring the concentration of hemoglobin in the filtrate using spectrophotometry [40]. Platelet activation will be tested by CD62 P (P-selectin) staining [41] of the retained cells, the filtrate and the membrane. The integrity of white blood cells in the system will be confirmed using a propidium iodide/acridine orange (PI/AO) stain [42].

Metrics for Success: We will validate this Aim when we: 1) can achieve a separation efficiency of 1:10,000 (0.01%) WBCs in the filtrate fraction and 2) can efficiently separate RBCs and platelets from the plasma component (10,000 fewer RBCs and platelets in the filtrate compared to whole blood) with insignificant platelet activation, red cell stress, or cell lysis compared to static controls.

Progress: We have shown that we can successfully separate the white blood cell fraction from whole blood using a 4 µm microslit filter with red blood cell clearance **(Figure 9b** and **9c**). However, the slit membranes were very large and a large number of WBCs were able to pass through to the filtrate. Furthermore, many RBCs became echinocytic (an indicator of stress), suggesting that the pressure may have been too high through the slits.

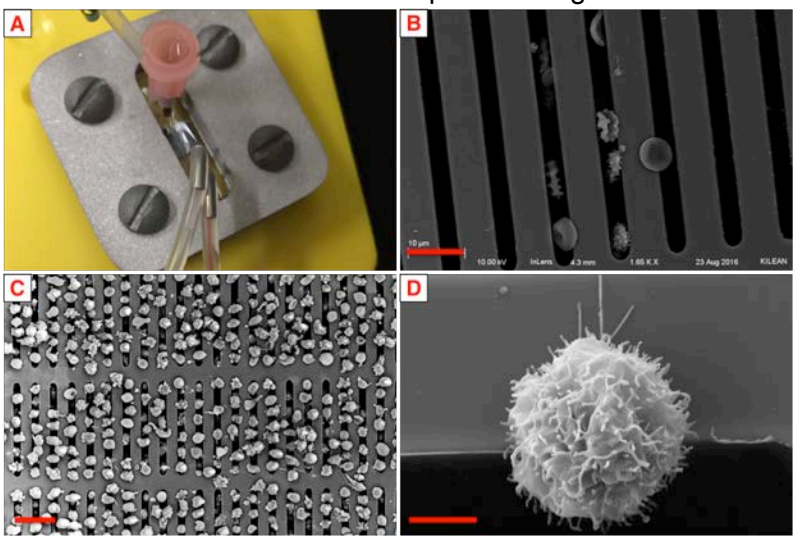

Figure 9: A) Microfluidic blood separation device showing red blood cells coming from the bottom outlet (right) and clear fluid/buffer coming from the top outlet (left). **B)** SEM of red blood cells passing through the slits of the membrane. Scale = 10 µm. **C)** Low magnification SEM of white blood cells captured by the slit nanomembrane. Scale = 10 µm. **D)** SEM of an intact white blood cell retained by the microslit membrane. Scale = 1 µm.

Conclusions: We can easily separate whole blood in small volumes using a microslit membrane design. We also show that the majority of WBCs remain on the topside of the membrane and are structurally intact (**Figure 9d**). However, the capture process appears to stress the RBCs, indicating that it is necessary to better tune the flow rates to provide the minimum amount of stress possible while providing efficient separation.

Remaining Work: In order to complete this Aim, we must: 1) fully quantify blood cell separation to achieve the 1:10,000 efficiency target and use the cell count to optimize the flow conditions for more efficient separation, 2) use 0.4 µm microslit filtration membranes to separate RBCs and platelets from plasma, 3) optimize flow conditions to provide low pressure flow (i.e. low shear stress through the slits) to maintain RBC integrity and minimize platelet activation.

Aim 2c: Demonstrate the ability to separate exosomes from undiluted human urine.

Plan: Human urine from healthy patients will be obtained with IRB approval from the lab of Dr. Carla Beckham (Department of Urology, URMC). Urinary exosomes will be isolated using the standard ultracentrifugation protocol and checked for common exosome markers (Tsg101, Alix, CD63) by Western blot. We will then determine the concentration in a raw urine sample using NTA. We will then capture the exosomes from 1 mL of raw urine using the conditions identified in **Aim 2a** for human plasma, with a goal of capturing > 75% of the urinary exosomes in a single pass over a membrane chip. For analysis, samples will be washed with 1x phosphate buffered saline (PBS) and either backwashed from the membrane for NTA concentration analysis or imaged *in situ* by SEM to determine pore occupancy and capture efficiency. The concentration of particles will be compared to the starting concentrations determined by NTA to confirm the capture efficiency.

Additionally, to determine the exosome purity, we will again perform XPS analysis of the captured exosomes to measure the contaminating protein layer thickness. Samples will be performed in triplicate for technical replicates as well as for biological replicates to account for donor variations in urinary protein levels. Highly pure exosomes will be defined as 10^{10} exosomes/µg protein [12], as with plasma-derived exosomes.

Expected Outcomes: At the completion of this aim, we expect to see similar capture to the plasma-derived samples, as the working fluid is very similar. While urine has a significant protein density (2 mg/mL [37]), it is still lower than plasma and thus it should be easier to purify exosomes from urine.

Challenges and Alternative Strategies:

Blood and urine are highly complex biofluids, which provide many challenges to the separation of exosomes from plasma/urine. The first challenge that presents itself is protein contamination of the pores. The high levels of protein that are present in blood (> 60 mg/mL [35]) can lead to significant fouling – and thus pore occlusion – that could result in lack of capture. If protein contamination is a problem however, we have developed methods to coat the membrane with a polyethylene glycol (PEG) layer [38]. This would create a non-adherent surface for protein and prevent adhesion-based capture of proteins and exosomes. We note that ~7 nm PEG coating only slightly reduces the dimensions of the pores and membranes retain their high permeability [38]. So we should not lose membrane functionality in our devices.

If the transmembrane pressure is too high during cell removal, then it is possible to lyse cells and contaminate the plasma sample. In addition to lysis, simply stressing the platelets can lead to activation [43], which may cause occlusion of the pores. Exosome production by platelets is also upregulated upon activation, which would cause dilution of any tumor-related exosome. Therefore, if there is too much stress on the cells, we will need to optimize the flow to provide the transmembrane pressure that is suitable for filtration.

A third challenge is the possibility of pore diameters being too large that flexible cells (e.g. RBCs and platelets) can still pass through. With enough pressure, it is possible to have RBCs pass through even 0.4 μm slits. There are two possible solutions to this problem however: 1) reduce the pressure (tied to the aforementioned lysis problem) and 2) reduce the pore diameter even further. In order to reduce the pore diameter, we can use atomic layer deposition (ALD) with platinum, alumina, or silica [44]. This technique allows for the precise addition of monolayers giving highly specific tuning to further control the pore dimensions.

Aim 3: Demonstrate the ability to identify cancer-derived exosomes from non-cancer exosomes *in situ* on a silicon nanomembrane.

Rationale: With the development of a tangential flow microfluidic device that can capture > 75% of the exosomes from a blood or urine sample, we seek to demonstrate the detection of tumor-derived exosomes *in situ* by identifying cancer specific markers with fluorescent tags. Typical methods of detection for proteins on exosomes involve immunoblot assays requiring large quantities of exosomes (100 μg of protein worth, ~ 10^{10} exosomes minimum) collected from more than 20 mL of fluid. Therefore, single exosome-level detection of protein biomarkers would significantly reduce the amount of sample and processing time. Furthermore, since cancer-derived exosomes represent a small fraction of the total number of exosomes (~ 1%) [8, 9], identifying biomarkers on individual exosomes should enable robust statistics from the counting of individual events rather than measurements on an ensemble. This is analogous to the advantages of using flow cytometry for cellular analysis rather than spectrophotometry that averages the solution properties.

Urine is an ideal biofluid choice for our proof-of-principle studies because it is easy to obtain, has low protein content, and because there are well-characterized exosome-associated markers of bladder cancer. For low-grade bladder cancer (LGBC) this marker is the protein mucin 2 (MUC2), found on exosomes derived from tumor cells and not on healthy cell derived exosomes [45]. By targeting this molecule with an immunostain (e.g. anti-MUC2 antibodies conjugated to gold nanoparticles or a fluorophore), we expect to be able to identify cancer specific exosomes from a diverse selection on a silicon nanomembrane.

Plan: Bladder cancer cell lines (e.g. 5637 (grade II), T24 (grade III), TCC-SUP (grade IV), and SV-HUC cells) expressing MUC2 (**Figure 10**) will be cultured by the Beckham lab. Primary bladder epithelium (PBE) cells will also be cultured as MUC2 negative controls. Exosomes will be harvested from the conditioned media by ultracentrifugation and then assayed for their expression levels of MUC2, which will be normalized to the protein GAPDH. The exosomes will also be characterized for expression of the standard exosome proteins (e.g. CD63, CD9, CD81) by Western blot and for size and concentration using NTA.

Exosomes purified from bladder cancer and PBE cell lines will be mixed in ratios of, 1:1,000, and 1:10,000 cancer to healthy exosomes at a concentration of 10^9 exosomes/mL. Then 1 mL of sample will be captured in the tangential flow microfluidic device (**Aim 2**) under the optimized conditions found in **Aim 1**. After capture, the nanomembrane chips will be labeled for MUC2 (Abcam, ab11197), removed and investigated by optical microscopy (fluorophore-tagged antibodies), SEM (20 nm gold-tagged antibodies) and TEM (20 nm gold-tagged antibodies). The limit of detection for MUC2 labeled antibodies will be determined for each assay.

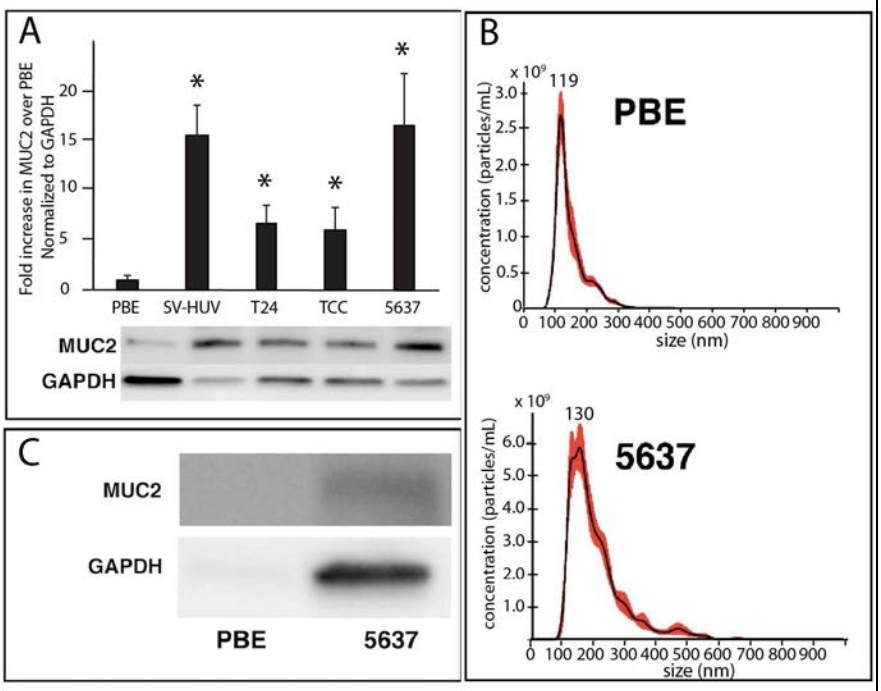

Figure 10: (A) Western blot of MUC2 and GAPDH from the cell lysates of primary bladder epithelial cells (PBE) or immortalized (SV-HUC) or bladder cancer cell lines (T24, TCC, 5637). A representative result is shown in lower panel, upper panel is the fold increase in MUC2 protein levels over PBEs, normalized to GAPDH (*T test p-value<0.05). (B) NanoSight analysis of purified exosomes from PBE and 5637 cells. Note the mode of the peak sizes are consistent with the expected exosome size indicating a pure sample. (C) Western blot of MUC2 and GAPDH from the purified exosomes of PBE and 5637 bladder cancer cell lines. For normalization, an equivalent number of exosomes and amount protein are loaded for each sample. Reference gene levels in exosomes and cell lysates depend on cell types.

Upon successful identification of MUC2 positive exosomes, the system will be tested using a blinded study. Ten samples containing both MUC2 positive and PBE derived exosomes as well as ten samples with only PBE derived exosomes will be prepared by the Beckham lab. These samples will then be isolated using the tangential flow microfluidic device and the identification procedure will be correlated to known results to eliminate bias.

Expected Outcomes: Exosome detection limits are expected to be a minimum of 1000 bladder cancer-derived exosomes on the membrane ($1:10^6$), with higher concentrations of cancer-derived exosomes providing easier detection. Additionally, we expect the specificity for MUC2 positive exosomes to be very high (minimal non-specific binding), providing high contrast to the PBE exosomes.

Challenges and Alternative Strategies: While MUC2 is known to be highly expressed in bladder cancer cells, it is likely that only a small fraction of the exosomes express MUC2. If this fraction proves too low for reliable detection, we may need to examine other BC biomarkers (such as EDIL-3) simultaneously to develop proof-of-principle.

Optical microscopy is limited in its ability to detect and resolve sub-micron particles. While individual exosomes are too far below the optical limit to be imaged with a conventional fluorescence or confocal microscope, it is known that individual exosomes contain multiple copies of surface proteins [46, 47], and so multiple fluorophores on multiple biomarker copies may provide strong signals. Another technique of increasing the signal would be to use quantum dots (QDs) rather than a fluorescent molecule as they are less susceptible to photobleaching, providing signal for significantly longer. To resolve individual exosomes, we plan to use either total internal reflection fluorescence (TIRF) microscopy or stimulated emission depletion (STED) super-resolution optical microscopy [48-50].

If markers are difficult to identify using optical or electron microscopy, we can remove exosomes through backwash and analyze miRNA content by RT-PCR. The Beckham lab has shown that the long

non-coding HOTAIR RNA is enriched in urinary exosomes and would be an ideal target for amplification and identification using qPCR [51, 52]. While some of the novelties of *in situ* capture and characterization would be lost in this case, we would still demonstrate the advantages of low sample volume requirements, low protein contamination, and facile operation compared to conventional methods.

Proposed Timeline: Progress has been made on **Aim 1** and the development of the mathematical and CFD models is expected to take 8 months. **Aim 2** has significant preliminary data and is expected to be worked on simultaneous to Aim 1 with an expected completion of 16-24 months. No progress has been made on **Aim 3**. It is expected that progress will be made near the end of **Aim 2** with an expected completion within 36 months.

References:

[1] N. A. Howlader N, Krapcho M, Miller D, Bishop K, Kosary CL, Yu M, Ruhl J, Tatalovich Z, Mariotto A, Lewis DR, Chen HS, Feuer EJ, Cronin KA (eds). SEER Cancer Statistics Review, 1975-2014 [Online].

[2] C. Hiley, E. C. de Bruin, N. McGranahan, and C. Swanton, "Deciphering intratumor heterogeneity and temporal acquisition of driver events to refine precision medicine," *Genome Biology,* vol. 15, no. 8, p. 453, 2014/08/27 2014.

[3] C. Swanton, "Intratumor Heterogeneity: Evolution through Space and Time," *Cancer Research,* 10.1158/0008-5472.CAN-12-2217 vol. 72, no. 19, p. 4875, 2012.

[4] C. D'Souza-Schorey and J. W. Clancy, "Tumor-derived microvesicles: shedding light on novel microenvironment modulators and prospective cancer biomarkers," *Genes & Development,* vol. 26, no. 12, pp. 1287-1299, 2012.

[5] J. Nilsson *et al.*, "Prostate cancer-derived urine exosomes: a novel approach to biomarkers for prostate cancer," *British Journal of Cancer,* vol. 100, no. 10, pp. 1603-1607

[6] A. V. Vlassov, S. Magdaleno, R. Setterquist, and R. Conrad, "Exosomes: Current knowledge of their composition, biological functions, and diagnostic and therapeutic potentials," *Biochimica et Biophysica Acta (BBA) - General Subjects,* vol. 1820, no. 7, pp. 940-948, 2012/07/01/ 2012.

[7] J. Ko, E. Carpenter, and D. Issadore, "Detection and isolation of circulating exosomes and microvesicles for cancer monitoring and diagnostics using micro-/nano-based devices," *Analyst,* 10.1039/C5AN01610J vol. 141, no. 2, pp. 450-460, 2016.

[8] X. Huang *et al.*, "Characterization of human plasma-derived exosomal RNAs by deep sequencing," *BMC Genomics,* vol. 14, no. 1, p. 319, 2013/05/10 2013.

[9] K. Rekker *et al.*, "Comparison of serum exosome isolation methods for microRNA profiling," *Clinical Biochemistry,* vol. 47, no. 1, pp. 135-138, 2014/01/01/ 2014.

[10] H. Kalra *et al.*, "Comparative proteomics evaluation of plasma exosome isolation techniques and assessment of the stability of exosomes in normal human blood plasma," *PROTEOMICS,* vol. 13, no. 22, pp. 3354-3364, 2013.

[11] R. J. Lobb *et al.*, "Optimized exosome isolation protocol for cell culture supernatant and human plasma," *Journal of Extracellular Vesicles,* vol. 4, p. 10.3402/jev.v4.27031

[12] J. Webber and A. Clayton, "How pure are your vesicles?," *Journal of Extracellular Vesicles,* vol. 2, p. 10.3402/jev.v2i0.19861

[13] L. Milane, A. Singh, G. Mattheolabakis, M. Suresh, and M. M. Amiji, "Exosome mediated communication within the tumor microenvironment," *Journal of Controlled Release,* vol. 219, no. Supplement C, pp. 278-294, 2015/12/10/ 2015.

[14] L. A. Mulcahy, R. C. Pink, and D. R. F. Carter, "Routes and mechanisms of extracellular vesicle uptake," *Journal of Extracellular Vesicles,* vol. 3, no. 1, p. 24641, 2014/01/01 2014.

[15] C. Théry, L. Zitvogel, and S. Amigorena, "Exosomes: composition, biogenesis and function," *Nature Reviews Immunology,* Review Article vol. 2, p. 569, 08/01/online 2002.

[16] D. Berger, "A brief history of medical diagnosis and the birth of the clinical laboratory. Part 1--Ancient times through the 19th century," (in eng), no. 0580-7247 (Print).

[17] R. Cazzoli *et al.*, "microRNAs Derived from Circulating Exosomes as Noninvasive Biomarkers for Screening and Diagnosing Lung Cancer," *Journal of Thoracic Oncology,* vol. 8, no. 9, pp. 1156-1162, 2013/09/01/ 2013.

[18] P. G. Moon *et al.*, "Identification of Developmental Endothelial Locus-1 on Circulating Extracellular Vesicles as a Novel Biomarker for Early Breast Cancer Detection," (in eng), no. 1078-0432 (Print).

[19] D. D. Taylor and C. Gercel-Taylor, "MicroRNA signatures of tumor-derived exosomes as diagnostic biomarkers of ovarian cancer," *Gynecologic Oncology,* vol. 110, no. 1, pp. 13-21, 2008/07/01/ 2008.

[20] A. G. van der Heijden and J. A. Witjes, "Recurrence, Progression, and Follow-Up in Non–Muscle-Invasive Bladder Cancer," *European Urology Supplements,* vol. 8, no. 7, pp. 556-562, 2009/09/01/ 2009.
[21] C.-L. Chen *et al.*, "Comparative and Targeted Proteomic Analyses of Urinary Microparticles from Bladder Cancer and Hernia Patients," *Journal of Proteome Research,* vol. 11, no. 12, pp. 5611-5629, 2012/12/07 2012.
[22] C. J. Beckham *et al.*, "Bladder Cancer Exosomes Contain EDIL-3/Del1 and Facilitate Cancer Progression," *The Journal of Urology,* vol. 192, no. 2, pp. 583-592, 2014/08/01/ 2014.
[23] D. A. Armstrong, B. B. Green, J. D. Seigne, A. R. Schned, and C. J. Marsit, "MicroRNA molecular profiling from matched tumor and bio-fluids in bladder cancer," *Molecular Cancer,* vol. 14, no. 1, p. 194, 2015/11/14 2015.
[24] T. Baranyai *et al.*, "Isolation of Exosomes from Blood Plasma: Qualitative and Quantitative Comparison of Ultracentrifugation and Size Exclusion Chromatography Methods," *PLOS ONE,* vol. 10, no. 12, p. e0145686, 2015.
[25] A. N. Böing, E. van der Pol, A. E. Grootemaat, F. A. W. Coumans, A. Sturk, and R. Nieuwland, "Single-step isolation of extracellular vesicles by size-exclusion chromatography," *Journal of Extracellular Vesicles,* vol. 3, p. 10.3402/jev.v3.23430
[26] D. Enderle *et al.*, "Characterization of RNA from Exosomes and Other Extracellular Vesicles Isolated by a Novel Spin Column-Based Method," *PLOS ONE,* vol. 10, no. 8, p. e0136133, 2015.
[27] F. Wu and T. J. Antes, "Abstract 3030: An exosome isolation system for serum-based cancer biomarker discovery," *Cancer Research,* 10.1158/1538-7445.AM10-3030 vol. 70, no. 8 Supplement, p. 3030, 2010.
[28] C. Lee *et al.*, "3D plasmonic nanobowl platform for the study of exosomes in solution," (in eng), no. 2040-3372 (Electronic).
[29] S. Mathivanan, J. W. E. Lim, B. J. Tauro, H. Ji, R. L. Moritz, and R. J. Simpson, "Proteomics Analysis of A33 Immunoaffinity-purified Exosomes Released from the Human Colon Tumor Cell Line LIM1215 Reveals a Tissue-specific Protein Signature," *Molecular & Cellular Proteomics : MCP,* vol. 9, no. 2, pp. 197-208
[30] R. T. Davies, J. Kim, S. C. Jang, E.-J. Choi, Y. S. Gho, and J. Park, "Microfluidic filtration system to isolate extracellular vesicles from blood," *Lab on a Chip,* 10.1039/C2LC41006K vol. 12, no. 24, pp. 5202-5210, 2012.
[31] C. Théry, S. Amigorena, G. Raposo, and A. Clayton, "Isolation and Characterization of Exosomes from Cell Culture Supernatants and Biological Fluids," in *Current Protocols in Cell Biology*: John Wiley & Sons, Inc., 2001.
[32] B. H. Wunsch *et al.*, "Nanoscale lateral displacement arrays for the separation of exosomes and colloids down to 20 nm," *Nature Nanotechnology,* vol. 11, p. 936, 08/01/online 2016.
[33] M. Logozzi *et al.*, "High Levels of Exosomes Expressing CD63 and Caveolin-1 in Plasma of Melanoma Patients," *PLOS ONE,* vol. 4, no. 4, p. e5219, 2009.
[34] M. L. Heinemann *et al.*, "Benchtop isolation and characterization of functional exosomes by sequential filtration," *Journal of Chromatography A,* vol. 1371, no. Supplement C, pp. 125-135, 2014/12/05/ 2014.
[35] J. R. Marrack and H. Hoch, "Serum Proteins: A Review," *Journal of Clinical Pathology,* vol. 2, no. 3, pp. 161-192, 1949.
[36] H. Lee and S. Balachandar, "Drag and lift forces on a spherical particle moving on a wall in a shear flow at finite Re," *Journal of Fluid Mechanics,* vol. 657, pp. 89-125, 2010.
[37] J. Adachi, C. Kumar, Y. Zhang, J. V. Olsen, and M. Mann, "The human urinary proteome contains more than 1500 proteins, including a large proportion of membrane proteins," *Genome Biology,* vol. 7, no. 9, pp. R80-R80
[38] X. Li *et al.*, "Modification of Nanoporous Silicon Nitride with Stable and Functional Organic Monolayers," *Chemistry of Materials,* vol. 29, no. 5, pp. 2294-2302, 2017/03/14 2017.

[39] D. M. Kanani, W. H. Fissell, S. Roy, A. Dubnisheva, A. Fleischman, and A. L. Zydney, "Permeability - Selectivity Analysis for Ultrafiltration: Effect of Pore Geometry," *Journal of membrane science,* vol. 349, no. 1-2, pp. 405-405, 2010.

[40] R. A. Malinauskas, "Plasma Hemoglobin Measurement Techniques for the In Vitro Evaluation of Blood Damage Caused by Medical Devices," *Artificial Organs,* vol. 21, no. 12, pp. 1255-1267, 1997.

[41] Y. Chen *et al.*, "High-throughput acoustic separation of platelets from whole blood," *Lab on a Chip,* 10.1039/C6LC00682E vol. 16, no. 18, pp. 3466-3472, 2016.

[42] X. Li, W. Chen, G. Liu, W. Lu, and J. Fu, "Continuous-flow microfluidic blood cell sorting for unprocessed whole blood using surface-micromachined microfiltration membranes," *Lab on a chip,* vol. 14, no. 14, pp. 2565-2575, 2014.

[43] P. A. Holme *et al.*, "Shear-Induced Platelet Activation and Platelet Microparticle Formation at Blood Flow Conditions as in Arteries With a Severe Stenosis," *Arteriosclerosis, Thrombosis, and Vascular Biology,* 10.1161/01.ATV.17.4.646 vol. 17, no. 4, p. 646, 1997.

[44] K. J. P. Smith, M. May, R. Baltus, and J. L. McGrath, "A predictive model of separations in dead-end filtration with ultrathin membranes," *Separation and Purification Technology,* vol. 189, no. Supplement C, pp. 40-47, 2017/12/22/ 2017.

[45] S. Stojnev *et al.*, "Prognostic significance of mucin expression in urothelial bladder cancer," *International Journal of Clinical and Experimental Pathology,* vol. 7, no. 8, pp. 4945-4958

[46] N. Arraud *et al.*, "Extracellular vesicles from blood plasma: determination of their morphology, size, phenotype and concentration," *Journal of Thrombosis and Haemostasis,* vol. 12, no. 5, pp. 614-627, 2014.

[47] J. L. Höög and J. Lötvall, "Diversity of extracellular vesicles in human ejaculates revealed by cryo-electron microscopy," *Journal of Extracellular Vesicles,* vol. 4, p. 10.3402/jev.v4.28680

[48] F. Persson, P. Bingen, T. Staudt, J. Engelhardt, J. O. Tegenfeldt, and S. W. Hell, "Fluorescence Nanoscopy of Single DNA Molecules by Using Stimulated Emission Depletion (STED)," *Angewandte Chemie International Edition,* vol. 50, no. 24, pp. 5581-5583, 2011.

[49] P. Bianchini, C. Peres, M. Oneto, S. Galiani, G. Vicidomini, and A. Diaspro, "STED nanoscopy: a glimpse into the future," *Cell and Tissue Research,* journal article vol. 360, no. 1, pp. 143-150, April 01 2015.

[50] C. Chen *et al.*, "Imaging and Intracellular Tracking of Cancer-Derived Exosomes Using Single-Molecule Localization-Based Super-Resolution Microscope," *ACS Applied Materials & Interfaces,* vol. 8, no. 39, pp. 25825-25833, 2016/10/05 2016.

[51] C. Berrondo *et al.*, "Expression of the Long Non-Coding RNA HOTAIR Correlates with Disease Progression in Bladder Cancer and Is Contained in Bladder Cancer Patient Urinary Exosomes," *PLOS ONE,* vol. 11, no. 1, p. e0147236, 2016.

[52] K. Junker, J. Heinzelmann, C. Beckham, T. Ochiya, and G. Jenster, "Extracellular Vesicles and Their Role in Urologic Malignancies," *European Urology,* vol. 70, no. 2, pp. 323-331, 2016/08/01/ 2016.